

# Litre-scale microbial fuel cells operated in a complete loop

Peter Clauwaert · Schalla Mulenga · Peter Aelterman · Willy Verstraete

Received: 13 October 2008 / Revised: 13 January 2009 / Accepted: 14 January 2009 / Published online: 29 January 2009  
© Springer-Verlag 2009

**Abstract** Using the anode effluent to compensate the alkalization in a bio-cathode has recently been proposed as a way to operate a microbial fuel cell (MFC) in a continuous and pH neutral way. In this research, we successfully demonstrated that the operation of a MFC without any pH adjustments is possible by completing the liquid loop over cathode and anode. During the complete loop operation, a stable current production of  $23.2 \pm 2.5 \text{ A m}^{-3} \text{ MFC}$  was obtained, even in the presence of  $3.2\text{--}5.2 \text{ mg O}_2 \text{ L}^{-1}$  in the anode. The use of current collectors and subdivided electrical circuitries for relative large 2.5-L-scale MFCs resulted in ohmic cell resistances in the order of  $1.4\text{--}1.7 \text{ m}\Omega \text{ m}^3 \text{ MFC}$ , which were comparable to values of ten times smaller MFCs. Nevertheless, the bio-cathode activity still needs to be improved significantly with a factor 10–50 in order achieve desirable current densities of  $1,000 \text{ A m}^{-3} \text{ MFC}$ .

**Keywords** Energy recovery · Bio-fuel cell · Bio-catalysed cathode · Bio-electrochemical system · Wastewater

## Introduction

Microbial fuel cells (MFCs) are a type of bio-electrochemical system in which chemical energy is converted into electrical power through microbial catalysis. Competitive current and

power productions of the order of  $2.1 \text{ kW m}^{-3} \text{ MFC}$  have been reported on a millilitre-scale reactor (Nevin et al. 2008), while scaling MFCs up to an industrial scale remains challenging (Clauwaert et al. 2008; Rozendal et al. 2008a). The largest sizes of MFCs that are reported in literature were between 0.52 and 1.27 L MFC. Typical volumetric current densities in these reactors were between 39 and  $103 \text{ A m}^{-3} \text{ MFC}$ , with power densities between 9 and  $32 \text{ W m}^{-3} \text{ MFC}$  (Clauwaert et al. 2007b; Freguia et al. 2008; Hong et al. 2008; Ter Heijne et al. 2007). The lower performance of larger microbial fuel cells is believed to be associated with higher ohmic voltage losses and higher electrode overpotentials (Clauwaert et al. 2008; Rozendal et al. 2008a).

One of the main challenges for MFCs is the operation without pH correction since the anode tends to acidify, while the cathode tends to become more alkaline due to slow and incomplete proton diffusion and migration through cation exchange membranes (Rozendal et al. 2006). Besides selecting membranes which retard the build-up of pH gradients (Rozendal et al. 2008b), a loop concept for MFCs has been presented where the anode effluent was used as the influent for the cathode (Freguia et al. 2008). As a result, the acidified anode effluent could compensate for the alkalization in the cathode and the pH in the cathode was between 7.1 and 7.3 (Freguia et al. 2008).

The oxygen reduction properties of graphite and carbon are limited, which implies that high cathode overpotentials limit the conversion rates and efficiencies in MFCs with catalyst-free cathodes. A bio-catalysed oxygen reduction was proposed as a sustainable cathode process in MFCs (Clauwaert et al. 2007b; Rabaey et al. 2008). The current and power production rates of MFCs with open-air bio-cathodes were in the same range of MFCs with platinum containing cathodes (Clauwaert et al. 2007b; Logan et al. 2007). Little is known about possible limiting factors in

**Electronic supplementary material** The online version of this article (doi:10.1007/s00253-009-1876-0) contains supplementary material, which is available to authorized users.

P. Clauwaert · S. Mulenga · P. Aelterman · W. Verstraete (✉)  
Laboratory of Microbial Ecology and Technology (LabMET),  
Ghent University,  
Coupure Links 653,  
9000 Ghent, Belgium  
e-mail: Willy.Verstraete@UGent.be

bio-cathodes like pH and dissolved oxygen (DO) gradients and whether it is possible to operate a MFC in which the effluent of a bio-anode serves as the influent for an oxygen-reducing bio-cathode while the cathode effluent serves as the anode influent (complete loop operation).

In this research, three MFCs (2.5 L each) with bio-anodes and open-air bio-cathodes (Clauwaert et al. 2007b) were constructed in a complete loop mode to evaluate the pH and dissolved oxygen profiles in the anodes and cathodes. The spatial contribution of the top, middle and bottom compartments of the reactor to the overall current production was evaluated. Finally, the limiting factors for this reactor were assessed.

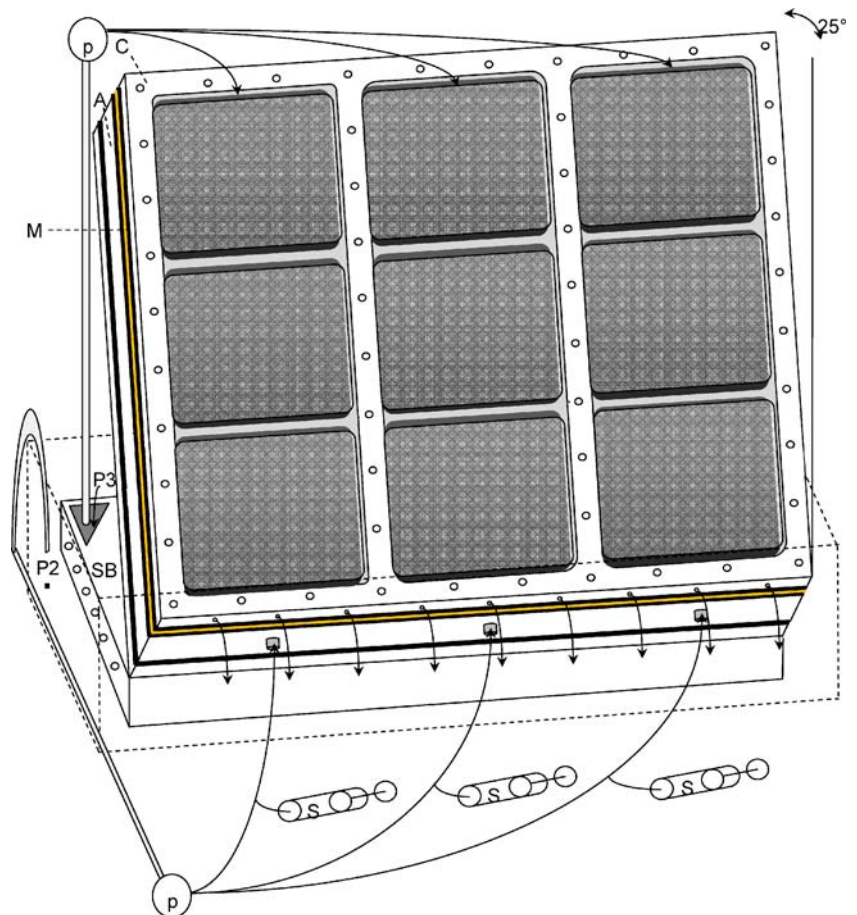
## Materials and methods

### Microbial fuel cell construction and operation

A plexiglass frame ( $53 \times 49 \times 3.2 \text{ cm}^3$ ) contained three anode lanes ( $15 \times 45 \times 3.2 \text{ cm}^3$ ), which could be subdivided in three equal parts by inserting perforated rubbers (Figure S1 of the supporting information). All nine subanodes were made of a  $15 \times 15 \times 3.2 \text{ cm}^3$  stainless steel frame (AISI 304L, De Coster

Manufacturing, Belgium) filled with granular graphite. A cation exchange membrane (Ultrex CMI7000, Membranes International, USA) was bolted between anode and cathode. The nine subcathodes consisted of  $14 \times 15 \times 0.5 \text{ cm}^3$  carbon felts (Sigratherm KFA, SGL Carbon group, Germany), which were kept in place with the help of  $14 \times 15 \text{ cm}^2$  stainless steel meshes (AISI 304L, De Coster Manufacturing, Belgium). As a result, the frame contained three MFCs with a volume of 2.5 L each or nine sub-MFCs with a volume of 0.833 L each. Graphite rods provided contact with the subanodes, while contact was made with the stainless steel mesh for the cathodes. The frame was mounted on a support box under an angle of  $25^\circ$  inside a liquid container (Fig. 1 and Figure S1 of the supporting information). The anodes were supplied with medium at the bottom of the lanes in an upstream mode ( $0.222 \text{ L h}^{-1}$ ), while the cathodic felts were humidified gravitational from the top of the lanes ( $0.8 \text{ L h}^{-1}$ ). A concentrated sodium acetate (Na-Ac) or acetic acid (H-Ac) solution was dosed at a rate of  $8.5 \text{ mL day}^{-1}$  just before the medium entered the anodic lanes in order to obtain the desired volumetric chemical oxygen demand (COD) loading rate. Inoculation of anodes and cathodes was performed as previously described (Clauwaert et al. 2007b). In a first phase, 10 L anode medium and 10 L cathode medium (6 g

**Fig. 1** Schematic overview of the reactor configuration and operation during loop operation (*A* the anode frame, *C* the cathode frame, *M* cation exchange membrane, *S* continuous syringe with concentrated substrate solution, *p* peristaltic pump, *SB* support box, *P2* and *P3* pH measurement points)



Na<sub>2</sub>HPO<sub>4</sub>·2H<sub>2</sub>O L<sup>-1</sup>, 3 g KH<sub>2</sub>PO<sub>4</sub> L<sup>-1</sup>, 1 g NaHCO<sub>3</sub> L<sup>-1</sup>, 0.2 g MgSO<sub>4</sub>·7H<sub>2</sub>O L<sup>-1</sup>, 0.1 g NH<sub>4</sub>Cl L<sup>-1</sup>, 0.0146 g CaCl<sub>2</sub> L<sup>-1</sup> and trace elements as previously described (Clauwaert et al. 2007b)) were separated by the cation exchange membrane (subsequently referred to as ‘not loop-operated; NL’), while in the next phase, the same type of medium (10 L) was used in the anode and the cathode (from here on ‘loop-operated; L’). The influent of the cathode was taken from underneath the perforated support box (indicated by P3, Fig. 1) on which the frame rested. The influent for the anodes was taken from point P2, as indicated in Fig. 1. The effluent of the anode lanes flowed into the support box (indicated by P3, Fig. 1). When the cells were not loop-operated, the pH in the anode recirculation vessel was at least adjusted daily to 7.0–7.5 by the addition of 1 N NaOH and the catholyte to 6.5–7.0 by addition of 1 N HCl. During loop operation with sodium acetate as the anodic substrate, the pH of the liquid was adjusted daily to 6.5–7 by addition of 1 N HCl. All tests were performed at room temperature (22±2°C).

Electrochemical measurements

The voltage was recorded every minute with a data acquisition unit (HP 34970A, Agilent) over a 10, 5 or 1.66 Ω resistor. The hourly averages were then used for further calculations. Polarisation curves (scan rate, 1 mV s<sup>-1</sup>) were obtained with the help of a potentiostat (PAR Bi-Stat Potentiostat, Princeton Applied Research, France). The ohmic cell resistance was determined with the current interrupt method based on the change of cell voltage after disconnecting the cell during a potentiostatic program. The potential of the cathodic electrodes was measured weekly with an Ag/AgCl reference electrode (assumed +0.197 V vs SHE; model RE-5B, BASi, United Kingdom), and the anode potential was calculated from the cathode potential, the cell voltage and the ohmic voltage drop.

Analytical measurements

Acetate concentrations of the anode effluents and at point P3 were determined three times per week as previously described (Clauwaert et al. 2007a). The pH was measured with a Consort C535 pH metre and the DO levels were measured with a Hach HQ30d flexi oxygen meter.

Results

Reactor performance

When the anode and cathode had a separate liquid recirculation and were thus NL, the average contribution of the upper parts of the cells to the current production (6.5–11.3 A m<sup>-3</sup> MFC)

**Table 1** Summary of the performance of ten tests in which sodium acetate (Na-Ac) or acetic acid (H-Ac) was the anodic substrate during not loop (NL) or loop (L) operation

Test	O. M.	Substrate	B <sub>v</sub> (kg COD m <sup>-3</sup> MFC day <sup>-1</sup> )	R <sub>ext</sub> (mΩ m <sup>3</sup> MFC)	Duration (day)	I (A m <sup>-3</sup> MFC)	i (A m <sup>-2</sup> )	CE (%)	COD removal (%)	P (W m <sup>-3</sup> MFC)	A (%)	B (%)	C (%)
1	NL	Na-Ac	0.09	8.3	14	6.5±2.3	0.26	54	n.d.	0.4±0.2	38±9	35±8	27±12
2	NL	Na-Ac	0.17	8.3	38	11.3±6.0	0.45	47	n.d.	1.4±1.6	43±13	34±8	23±9
3	NL	Na-Ac (Spike-fed)		8.3	18	29.1±10.4	1.15	n.d.	n.d.	7.9±4.7	35±4	44±7	21±7
4	NL	Na-Ac (Spike-fed)		4.2	17	29.1±10.4	1.15	n.d.	n.d.	4.0±2.5	33±6	43±11	24±9
5	L	Na-Ac	0.14	4.2	13	13.9±5.8	0.55	69	97±2	0.9±0.7	25±8	44±10	31±13
6	L	Na-Ac	0.23	4.2	10	20.9±6.1	0.83	65	89±10	2.0±1.1	28±7	39±7	33±7
7	L	Na-Ac	0.32	4.2	7	21.6±5.4	0.86	49	85±10	2.1±1.0	34±8	35±7	31±7
8	L	H-Ac	0.32	4.2	10	22.0±5.1	0.87	50	73±19	2.1±0.9	39±7	33±4	27±3
9	L <sup>a</sup>	H-Ac	0.32	4.2	13	23.2±2.5	0.92	52	81±18	2.3±0.5	<sup>b</sup>	<sup>b</sup>	<sup>b</sup>
10	L <sup>c</sup>	H-Ac	0.32	4.2	10	10.9±3.0	0.43	24	n.d.	0.5±0.3	34±6	33±6	33±4

The contribution (percent) to the current production of the upper (a), middle (b) and bottom (c) subcells are indicated. The standard deviation for i and CE are proportional to the standard deviation of I

O.M. operation mode, B<sub>v</sub> volumetric COD loading rate, R<sub>ext</sub> external resistance, I volumetric current production, i specific current production expressed per projected cathode surface, CE coulombic efficiency, P volumetric power production, n.d. not determined

<sup>a</sup>Three subcells a, b and c connected in parallel over one external resistor for every MFC

<sup>b</sup>Not applicable

<sup>c</sup>Cathodes autoclaved prior to the test

**Table 2** Summary of the polarisation tests (scan rate,  $1 \text{ mV s}^{-1}$ ) obtained during not loop (NL) and loop (L) operation with sodium acetate (Na-Ac) or acetic acid (H-Ac) as the substrate

Operation mode	Substrate	$B_v$ ( $\text{kg COD m}^{-3} \text{ MFC day}^{-1}$ )	$I_{ssc}^{av}$ ( $\text{A m}^{-3} \text{ MFC}$ )	$I_{ssc}^{max}$ ( $\text{A m}^{-3} \text{ MFC}$ )	$P_{peak}^{av}$ ( $\text{W m}^{-3} \text{ MFC}$ )	$P_{peak}^{max}$ ( $\text{W m}^{-3} \text{ MFC}$ )
NL	Na-Ac	(Spike-fed)	$42.1 \pm 15.3$	81.4	$7.8 \pm 4.6$	17.4
L	Na-Ac or H-Ac	0.32	$34.1 \pm 10.9$	54.2	$6.5 \pm 3.8$	13.2
La	H-Ac	0.32	$42.1 \pm 5.4$	48.3	$9.8 \pm 2.5$	14.5

The open circuit voltage plotted vs the peak power production is represented in Fig. 2

$B_v$  volumetric COD loading rate,  $I_{ssc}^{av}$  the average short circuit current,  $I_{ssc}^{max}$  the maximum short circuit current,  $P_{peak}^{av}$  the average peak power production,  $P_{peak}^{max}$  the maximum peak power production

<sup>a</sup> Three subcells *a*, *b* and *c* connected in parallel for every MFC

was in the order of 40%, that of the lower parts of the cells was around 25% (Table 1, Tests 1 and 2). When the operation was switched to a spike feeding regime (10 g sodium acetate), as a way to evaluate the operation under optimal anode feeding conditions (Table 2, Tests 3 and 4), the current production increased up to  $29.1 \pm 10.4 \text{ A m}^{-3} \text{ MFC}$  with a maximum of  $50.4 \text{ A m}^{-3} \text{ MFC}$ . The average contribution of the lower parts of the cells to the current production was still lower than the upper parts of the cells. However, the middle cells had the highest performance. Lowering the external resistance from 10 to  $5 \Omega$  ( $8.3$  to  $4.2 \text{ m}\Omega \text{ m}^3 \text{ MFC}$ ) did not result in a higher current production and lowered the power production due to a lower cell voltage (Table 1).

In the next phases, the anodes and cathodes had a common liquid recirculation (L) and the reactor was operated under a continuous feeding regime. The volumetric COD loading rate was increased from 0.14 to  $0.32 \text{ kg COD m}^{-3} \text{ MFC day}^{-1}$  in the subsequent tests (Table 1, Tests 5–7). The average contribution to the current remained the highest for the middle parts of the cells. If acetic acid was supplied instead of sodium acetate, the cell performance was not significantly affected (Table 1, Test 8). Operating the three parts of the cell in parallel over one resistor did not result in a decrease of the cells performance (Table 1, Test 9). Just before test 10, the cathode felts were autoclaved and reconnected to the cell as a way to determine the contribution of microbial catalysis vs chemical oxygen reduction. The current production decreased with more than 50% and the difference in contribution to the current production for all parts of the cell became minimal (Table 1, Test 10).

On a weekly basis, polarisation curves were obtained from every subcell. A similar performance could be obtained during loop operation compared to not loop operation (Table 2). When the open circuit voltage (OCV) was lower than 0.5 V, the peak power production during polarisation was typically below  $5 \text{ W m}^{-3} \text{ MFC}$  (Fig. 2), and the cathode potentials in open circuit mode were typically between  $-0.170$  and  $+0.090 \text{ V vs SHE}$ . When the OCV was higher than 0.5 V, the cathode potential in open circuit mode was typically

between  $+0.400$  and  $+0.530 \text{ V vs SHE}$ , indicating an active bio-cathode, although intermediate cathode potentials (between  $+0.100$  and  $+0.400 \text{ V vs SHE}$ ) were also measured, indicating that a bio-cathode was not fully active at that time. The average cathode potential during loop operation (70 days) was  $-0.098 \pm 0.133 \text{ V vs SHE}$ , while the average anode potential was  $-0.219 \pm 0.074 \text{ V vs SHE}$  ( $R_{ext} = 4.2 \text{ m}\Omega \text{ m}^3 \text{ MFC}$ ).

The average ohmic cell resistance of all subcells was  $1.99 \pm 0.62 \Omega$ , corresponding with  $1.66 \pm 0.51 \text{ m}\Omega \text{ m}^3 \text{ MFC}$ , in the case of ‘non-loop’ operation, and it was  $1.73 \pm 0.60 \Omega$ , corresponding with  $1.44 \pm 0.50 \text{ m}\Omega \text{ m}^3 \text{ MFC}$ , in the case of ‘loop’ operation. When the three subcells were operated in parallel, the ohmic cell resistance was  $0.64 \pm 0.08 \Omega$ , corresponding with  $1.60 \pm 0.20 \text{ m}\Omega \text{ m}^3 \text{ MFC}$ .

#### pH and DO gradients

When the anodes and cathodes had separate liquid streams (NL-mode), there was a continuous decrease of the anolyte pH over time, while the catholyte pH increased (Table 3). These changes in pH needed to be counteracted with the supply of base and acid, respectively. When the loop

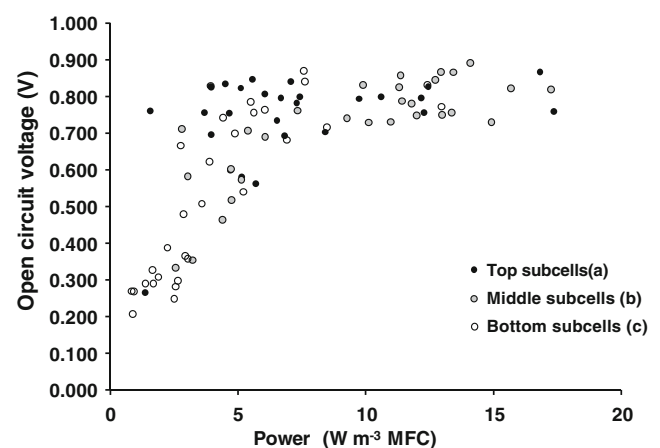


**Fig. 2** The OCV plotted vs the peak power production of polarisation curves of the different subcells as reported in Table 2

**Table 3** Overview of pH changes per day at three points (P1: the anode recirculation vessel; P2 and P3: see Fig. 1)

Operation mode	Substrate	Units of pH change day <sup>-1</sup>			pH values			
		P1	P2	P3	Anode in	Anode out	Cathode in	Cathode out
NL	Na-Ac	-1.0±0.3	+1.5±0.6	+1.0±0.5	n.d.	n.d.	n.d.	n.d.
L	Na-Ac	-a	+0.5±0.2	+0.2±0.1	7.3±0.4	7.0±0.1	7.2±0.2	7.6±0.1
L	H-Ac	-a	+0.0±0.1	+0.0±0.1	7.5±0.1	6.9±0.1	7.4±0.1	7.7±0.3

Anode acidification was adjusted with 1 M NaOH; cathode alkalization was adjusted with 1 N HCl. When acetic acid (H-Ac) was used, no pH adjustment was needed

*n.d.* not determined

<sup>a</sup> Not applicable

operation was applied, the acidification of the anode was supposed to neutralise the alkalization of the cathode. Nevertheless, the overall pH still increased when feeding sodium acetate. However, when acetic acid was used as the anodic substrate, no pH adjustments were needed anymore and a constant pH was found (Table 3).

In the NL operation mode, the catholyte was not aerated, and the DO level was  $5.8 \pm 0.3 \text{ mg O}_2 \text{ L}^{-1}$ , while the DO level was below  $0.1 \text{ mg O}_2 \text{ L}^{-1}$  in the anolyte. When the operation was switched to the loop mode, it was necessary to provide aeration (point P3, Fig. 1) because the COD removal after passage through the anode was incomplete (Table 1). In this way, a complete conversion of the substrate by aerobic heterotrophs was established outside the anodes. Due to the aeration, the DO level was around  $8.5 \text{ mg O}_2 \text{ L}^{-1}$  before it was used to humidify the cathodes (L-mode). The DO level decreased while flowing over the cathode and further decreased while passing through the anode. This profile was even more pronounced when the COD loading rate was increased (Fig. 3).

In a separate test, in which the aeration was stopped and the substrate was fed at  $0.32 \text{ kg acetic acid-COD m}^{-3} \text{ MFC day}^{-1}$ , the current production slowly decreased from  $17.8 \pm$

$4.9$  to  $9.7 \pm 4.3 \text{ A m}^{-3} \text{ MFC}$  over a period of 6 days during which the dissolved oxygen level in the collection box gradually decreased from  $8.5$  to  $0.9 \text{ mg O}_2 \text{ L}^{-1}$ .

## Discussion

In this study, litre-scale microbial fuel cells were constructed. The stable and pH neutral operation in a complete loop mode was demonstrated. The activity and the contribution of the subunits to the overall performance of the cell could be evaluated. A stable current production of about  $20 \text{ A m}^{-3} \text{ MFC}$  could be achieved, while the power production was typically between  $2$  and  $10 \text{ W m}^{-3} \text{ MFC}$ . The difference in performance compared to millilitre-sized MFCs, which generate electrical power densities up to  $2.1 \text{ kW m}^{-3} \text{ MFC}$  (Nevin et al. 2008), can be attributed to either a higher ohmic cell resistance, higher anode overpotentials, higher cathode overpotentials or a combination of these losses (Clauwaert et al. 2008). Longer charge paths for both ions and electrons and more contact points can be expected to increase the ohmic voltage loss when increasing the MFCs size. However, the ohmic cell resistance was not found to be the main limiting factor. The combination of current collectors in anodes and cathodes (subcircuits and stainless steel meshes) resulted in an ohmic resistance between  $1.4$  and  $1.7 \text{ m}\Omega \text{ m}^3 \text{ MFC}$ , which was in the same range as values reported for better performing  $0.2$ – $0.7$ -L-sized MFCs ( $1$ – $2 \text{ m}\Omega \text{ m}^3 \text{ MFC}$ ) with electrolytes with similar ionic strengths (Clauwaert et al. 2008).

A spiked feeding of the anodes with acetate, which is a strategy to minimise substrate associated concentration overpotentials, did not enhance the current production to levels that were much higher compared to a continuous substrate feeding. The average anode potential was  $-0.219 \pm 0.074 \text{ V}$  vs SHE, which demonstrates that the system was not limited by high anode overpotentials. In this research, it was found that at a volumetric COD loading rate of  $0.32 \text{ kg COD m}^{-3} \text{ MFC day}^{-1}$  (calculated anode influent concentration  $0.149 \text{ g COD L}^{-1}$ , Test 9, Table 1), the dissolved oxygen level dropped

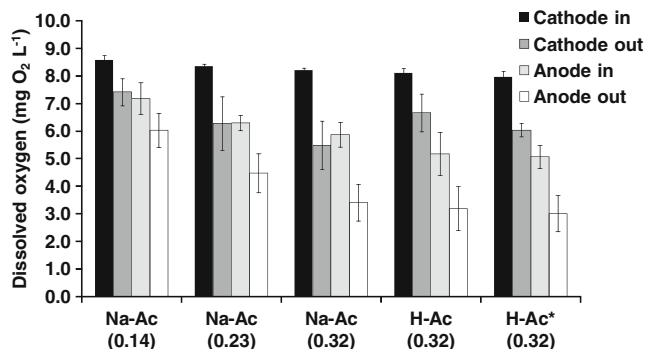


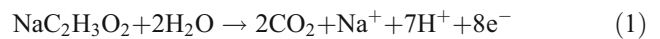
**Fig. 3** DO levels before and after passage through the anodes and cathodes when sodium acetate (*Na-Ac*) or acetic acid (*H-Ac*) was used as a substrate. The volumetric COD loading rates, expressed in kilograms COD per cubic metre MFC per day, are indicated between brackets (asterisk three subcells *a*, *b* and *c* connected in parallel for every MFC)

from  $5.2 \pm 0.8$  to  $3.2 \pm 0.8$  mg O<sub>2</sub> L<sup>-1</sup> during 6.2 h contact time (calculated hydraulic retention time). Surprisingly, this did not restrict the current production. The coulombic efficiency was around 50%, while the COD removal efficiency was  $81 \pm 18\%$ . The lowering of the dissolved oxygen level from the anode influent due to aerobic conversion of substrate cannot be put forward as the main cause. Biomass build-up and carbon storage, sulphate reduction, methanogenesis and oxygen intrusion through the membrane might have simultaneously accounted for this difference (Freguia et al. 2007; Logan et al. 2006). However, with the same membrane, coulombic efficiencies higher than 90% were reported (Clauwaert et al. 2007b; Rabaey et al. 2005) in reactors that even had a higher specific membrane surface installed compared to this reactor (69 vs 25 m<sup>2</sup> membrane m<sup>-3</sup> MFC). Further research is needed to investigate the effect of oxygen on the anodophilic conversion of organic compounds.

The average cathode potential was  $-0.098 \pm 0.133$  V vs SHE when the external resistance was 4.2 mΩ m<sup>3</sup> MFC, which means that the cathode overpotentials were dominant because the equilibrium potential of active bio-cathodes was found to be typically between +0.400 and +0.530 V vs SHE. These high overpotentials apparently limited the overall performance of the reactor. The bio-cathode performance has been described to be highly dependent on the recirculation rate of passively aerated bio-cathodes (Freguia et al. 2008). In general, the lower subcells were contributing the least to the current production, which is consistent with the finding that a low OCV and cathode potential are more associated with these subcells (Table 1 and Fig. 2), indicating no or a low bio-cathode activity (Clauwaert et al. 2007b). Sharp gradients of pH and dissolved oxygen levels between the bio-catalytic sites and the bulk solution, as well as low levels of cathodically formed hydrogen peroxide (Bond and Lovley 2003; Clauwaert et al. 2008; Zhao et al. 2005), are possible environmental factors suppressing the bio-cathode activity. Applying high shear rates to bio-cathodes might not only circumvent some of these limiting factors but it might also result in denser and thicker bio-films as was demonstrated for anodophilic bio-films (Pham et al. 2008). The introduction in the cathode of electron shuttling compounds produced in the anode might have a bacteriostatic effect (e.g. phenazines) or a positive effect if these electron mediators could be used for bio-cathodic electron transfer. Clearly, the mechanisms for electron transfer in bio-cathodes need to be better understood in order to increase the bio-cathode activity with at least a factor 50.

In this complete loop-operated set-up, the MFCs were operated with a continuous substrate feeding, while the electrolyte remained the same in order to avoid masked pH effects by a pH buffered effluent. pH stability could only be

demonstrated when acetic acid was dosed and not when sodium acetate was the electron donor. Indeed, dosing sodium acetate to a closed system for oxidation has an alkalinizing effect because in the anodes only 7 mol protons can be produced per 8 mol electrons, while an equimolar amount of protons and electrons are consumed in oxygen-reducing cathodes (Eq. 1).



In this study, we have demonstrated that an overall pH neutral operation without pH adjustments is possible. However, pH gradients over anodes and cathodes, over the membrane and between electrodes and bulk solutions cannot be prevented by this loop operation, and the fact that these gradients would even become larger using waters that are not strongly pH buffered makes implementation of MFCs on an industrial scale challenging (Rozendal et al. 2008a).

In this research, it was found that differences in MFC performance can occur according to the spatial localisation of subcells in a MFC. When enlarging the MFC volume to the litre scale, it is possible to keep the ohmic cell resistance at the same level as for millilitre-scale MFCs by introducing current collectors. However, economical optimisation of current collector systems is desired. Increasing the size of bio-cathodes resulted in increased cathode overpotentials. Further optimisation of bio-cathodes is required.

**Acknowledgements** The useful comments of Gabriele Gross and David van der Ha are kindly acknowledged. This research was funded by a Ph.D. grant (IWT grant 53305) of the Institute for the Promotion of Innovation through Science and Technology in Flanders (IWT-Vlaanderen) and the European Commission (Neptune project, contract no. 036845, FP6-2005-Global-4, SUSTDEV-2005-3.II.3.2).

## References

- Bond DR, Lovley DR (2003) Electricity production by *Geobacter sulfurreducens* attached to electrodes. *Appl Environ Microbiol* 69:1548–1555
- Clauwaert P, Rabaey K, Aelterman P, DeSchampelaire L, Pham TH, Boeckx P, Boon N, Verstraete W (2007a) Biological denitrification in microbial fuel cells. *Environ Sci Technol* 41:3354–3360
- Clauwaert P, Van der Ha D, Boon N, Verbeken K, Verhaege M, Rabaey K, Verstraete W (2007b) Open air biocathode enables effective electricity generation with microbial fuel cells. *Environ Sci Technol* 41:7564–7569
- Clauwaert P, Aelterman P, Pham TH, De Schampelaire L, Carballa M, Rabaey K, Verstraete W (2008) Minimizing losses in bio-electrochemical systems: the road to applications. *Appl Microbiol Biotechnol* 79:901–913
- Freguia S, Rabaey K, Yuan ZG, Keller J (2007) Electron and carbon balances in microbial fuel cells reveal temporary bacterial storage behavior during electricity generation. *Environ Sci Technol* 41:2915–2921
- Freguia S, Rabaey K, Yuan ZG, Keller J (2008) Sequential anode-cathode configuration improves cathodic oxygen reduction and effluent quality of microbial fuel cells. *Water Res* 42:1387–1396

- Hong L, Shaoan C, Liping H, Logan BE (2008) Scale-up of membrane-free single-chamber microbial fuel cells. *J Power Sources* 179:274–279
- Logan BE, Hamelers B, Rozendal R, Schroder U, Keller J, Freguia S, Aelterman P, Verstraete W, Rabaey K (2006) Microbial fuel cells: methodology and technology. *Environ Sci Technol* 40:5181–5192
- Logan BE, Cheng S, Watson V, Estadt G (2007) Graphite fiber brush anodes for increased power production in air-cathode microbial fuel cells. *Environ Sci Technol* 41:3341–3346
- Nevin KP, Richter H, Covalla SF, Johnson JP, Woodard TL, Orloff AL, Jia H, Zhang M, Lovley DR (2008) Power output and coulombic efficiencies from biofilms of *Geobacter sulfurreducens* comparable to mixed community microbial fuel cells. *Environ Microbiol* 10(10):2505–2514
- Pham H, Boon N, Aelterman P, Clauwaert P, De Schampelaire L, van Oostveldt P, Verbeken K, Rabaey K, Verstraete W (2008) High shear enrichment improves the performance of the anodophilic microbial consortium in a microbial fuel cell. *Microb Biotechnol* 1(6):487–496
- Rabaey K, Clauwaert P, Aelterman P, Verstraete W (2005) Tubular microbial fuel cells for efficient electricity generation. *Environ Sci Technol* 39:8077–8082
- Rabaey K, Read ST, Clauwaert P, Freguia S, Bond PL, Blackall LL, Keller J (2008) Cathodic oxygen reduction catalyzed by bacteria in microbial fuel cells. *Isme J* 2:519–527
- Rozendal RA, Hamelers HVM, Buisman CJN (2006) Effects of membrane cation transport on pH and microbial fuel cell performance. *Environ Sci Technol* 40:5206–5211
- Rozendal RA, Hamelers HVM, Rabaey K, Keller J, Buisman CJN (2008a) Towards practical implementation of bioelectrochemical wastewater treatment. *Trends Biotechnol* 26:450–459
- Rozendal RA, Sleutels T, Hamelers HVM, Buisman CJN (2008b) Effect of the type of ion exchange membrane on performance, ion transport, and pH in biocatalyzed electrolysis of wastewater. *Water Sci Technol* 57:1757–1762
- Ter Heijne A, Hamelers HVM, Buisman CJN (2007) Microbial fuel cell operation with continuous biological ferrous iron oxidation of the catholyte. *Environ Sci Technol* 41:4130–4134
- Zhao F, Harnisch F, Schroder U, Scholz F, Bogdanoff P, Herrmann I (2005) Application of pyrolysed iron(II) phthalocyanine and CoTMPP based oxygen reduction catalysts as cathode materials in microbial fuel cells. *Electrochem Commun* 7:1405–1410